Hindawi
International Journal of Mathematics and Mathematical Sciences
Volume 2023, Article ID 6620669, 17 pages
https://doi.org/10.1155/2023/6620669

Research Article

A Numerical Approach for Diffusion-Dominant Two-Parameter Singularly Perturbed Delay Parabolic Differential Equations

Solomon Woldu Worku [1] **and Gemechis File Duressa** [2]

[1] *Department of Mathematics, College of Natural Sciences, Arba Minch University, Arba Minch, Ethiopia*
[2] *Department of Mathematics, College of Natural Sciences, Jimma University, Jimma, Ethiopia*

Correspondence should be addressed to Solomon Woldu Worku; prns-011-12@amu.edu.et

Received 24 March 2023; Revised 5 December 2023; Accepted 9 December 2023; Published 27 December 2023

Academic Editor: Hans Engler

A numerical scheme is developed to solve a large time delay two-parameter singularly perturbed one-dimensional parabolic problem in a rectangular domain. Two small parameters multiply the convective and diffusive terms, which determine the width of the left and right lateral surface boundary layers. Uniform mesh and piece-wise uniform Shishkin mesh discretization are applied in time and spatial dimensions, respectively. The numerical scheme is formulated by using the Crank–Nicolson method on two consecutive time steps and the average central finite difference approximates in spatial derivatives. It is proved that the method is uniformly convergent, independent of the perturbation parameters, where the convection term is dominated by the diffusion term. The resulting scheme is almost second-order convergent in the spatial direction and second-order convergent in the temporal direction. Numerical experiments illustrate theoretical findings, and the method provides more accurate numerical solutions than prior literature.

1. Introduction

Most mathematical models of real-life phenomena in physics, chemistry, biology, astronomy, and other fields of applied science involve the dependent variable and its derivatives as arguments in the equation. In many cases, the higher-order terms are multiplied by "small" interrelated multiparameters, which are referred to as singularly perturbed differential equations. If we consider two perturbation parameters, one (say μ) can be assumed to be a function of the other (say ε). The earliest and popular paper [1] introduces these problems as two-parameter singularly perturbed differential equations defined as

$$\varepsilon \mathscr{L}_1 \varphi + \mu \mathscr{L}_2 \varphi + \mathscr{L}_3 \varphi = 0, \tag{1}$$

where ε and μ are "small" positive interrelated parameters simultaneously approaching zero and $\mathscr{L}_1$, $\mathscr{L}_2$, and $\mathscr{L}_3$ are linear differential operators whose orders are $l_1 > l_2 > l_3$, respectively, for a sufficiently smooth function φ. These kinds of equations arise in the fields of fluid dynamics, quantum mechanics, chemical flow reactor theory, and DC motor analysis [2, 3].

The two-parameter singularly perturbed parabolic differential equation is the focus of some recent studies [4–11]. Some others considered this problem with nonsmooth data, which implies boundary and interior layers in their solution [12–16]. However, they did not consider the delay condition. In other models of physical problems like heat and mass transfer, control theory, and chemical processes, the system may depend on the present and past history of the state which yields a delay term in the differential equation. Such singularly perturbed time delay parabolic problems with uniperturbation parameter are addressed by some literature [17–23]. Besides solving singularly perturbed differential equations, obtaining higher-order and robust numerical solutions is the main devotion of researchers [24–30].

The concern of our problem is a two-parameter singularly perturbed time delay one-dimensional parabolic differential equation for the given initial and two boundary conditions.

Different numerical methods of this type of problems are studied by some authors [31–34]. Govindarao and others in [31] solved the problem by applying implicit Euler finite difference approximation on uniform mesh in the direction of time and upwind finite difference approximation on Shishkin and Bakhvalov–Shishkin mesh in space direction. They proved that their scheme is parameter-uniform with $\mathcal{O}(h+k)$ where h and k are spatial and temporal mesh sizes. Kumar and Others in [32] improved the spatial order of convergence to almost second by implementing a hybrid monotone finite difference scheme in the direction of space. Recently, two articles entitled "An effective numerical approach for two-parameter time-delayed singularly perturbed problems" and "Fitted cubic spline scheme for two-parameter singularly perturbed time-delay parabolic problems" also addressed this problem. The first article applied the Crank–Nicolson scheme in temporal direction and the B-spline collocation method for spatial [33] and the second article applied a combination of the fitted operator scheme of a cubic spline with θ—method on a uniform mesh grid [34].

The properties of the solution to these problems mainly depend on the dominant of diffusive or convective parameter. The problem has a reaction-diffusion problem property and is referred to as diffusion-dominant if the convective parameter is significantly smaller than the diffusive parameter. This paper proposes to develop a more accurate and parameter-uniform numerical scheme to solve a two-parameter singularly perturbed one-dimension delay parabolic problem using the Crank–Nicolson finite difference approximation on a uniform mesh in the time direction and the central finite difference method on Shishkin mesh in the spatial direction when the diffusive parameter dominates the convective parameter.

This article consists of the following structures: in Section 2, the governing problem will be stated and the appropriate regularity of the analytical solution will be discussed. Section 3 discusses some prior bounds of the analytical solution and its derivatives. The discretization of the domain and development of the numerical scheme are presented in Section 4. Section 5 contains the stability and convergence analysis of the scheme. Section 6 strengthens theoretical results using numerical solutions of counterexamples with tables and graphs, and finally, a brief conclusion is given in Section 7.

In every part of this article, $\|.\|$ denotes the supreme norm, $\|f(x,t)\| = \sup_{(x,t)\in\overline{D}}\{|f(x,t)|\}$ if $f(x,t)$ is a continuous function defined on $\overline{D}$, and $\|f_{i,j}\| = \max_{1\le i\le N1\le j\le M}|f(x_i,t_j)|$ if $f_{i,j}$ is a discrete value on the tensor of the domain, where $N\times M$ is the discrete parameter. C denotes the generic positive constant independent of perturbation parameters and mesh sizes. The Landau symbol $\mathcal{O}$ is used to indicate order relations.

2. Statement of the Problem

We consider the two-parameter singularly perturbed large time delay one-dimensional parabolic problem defined on the rectangular domain

$$\begin{aligned}&\mathcal{D} = \mathcal{D}_x \times \mathcal{D}_t, \text{for } \mathcal{D}_x = (0,1),\\ &\mathcal{D}_t = (0,T],\end{aligned} \tag{2}$$

given by

$$\begin{aligned}&u_t(x,t) - \varepsilon u_{xx}(x,t) - \mu a(x,t)u_x(x,t) + b(x,t)u(x,t)\\ &\quad = c(x,t)u(x,t-\tau) + f(x,t),\end{aligned} \tag{3}$$

with initial and boundary conditions

$$\begin{cases} u(x,t) = \gamma_b(x,t), & (x,t)\in\Gamma_b = [0,1]\times[-\tau,0],\\ u(x,t) = \gamma_l(t), & (x,t)\in\Gamma_l = \{(0,t)\colon 0\le t\le T\},\\ u(x,t) = \gamma_r(t), & (x,t)\in\Gamma_r = \{(1,t)\colon 0\le t\le T\},\end{cases} \tag{4}$$

where ε and μ are perturbation parameters such that $0<\varepsilon\ll 1$ and $0<\mu\ll 1$, the delay parameter $\tau>\varepsilon,\mu$, such that the terminal time, $T = k\tau$ for some positive integer k. The functions $a(x,t), b(x,t), c(x,t)$, and $f(x,t)$ are sufficiently smooth and bounded that satisfy

$$\begin{aligned}&a(x,t)\ge\alpha>0, b(x,t)\ge\beta>0,\\ &c(x,t)\ge\vartheta>0 \text{ on } \overline{\mathcal{D}} = [0,1]\times[0,T],\end{aligned} \tag{5}$$

assuming that $\gamma_b(x,t), \gamma_l(t)$, and $\gamma_r(t)$ are sufficiently smooth and bounded on the boundary, $\Gamma = \Gamma_b\cup\Gamma_l\cup\Gamma_r$ and compatible at the corner points.

For $(x,t)\in[0,1]\times[0,\tau]$, the problem is treated as a standard two-parameter singularly perturbed parabolic problem since the value $u(x,t-\tau)$ is known. The computation extends for $(x,t)\in[0,1]\times[\tau,2\tau]$ after solving $u(x,t)$ for $[0,1]\times[0,\tau]$. Repeating this method of steps completes the solution for the whole time domain component.

The problem is a kind of reaction-diffusion when $\mu=0$ and convection-diffusion when $\mu=1$, but our interest is in the case $0<\mu\ll 1$. The analysis was made concerning two cases of O'Malley's study in [1], when $\mu^2\le C\varepsilon$ and $\mu^2\ge C\varepsilon$. In the first case, the problem resembles the properties of the case when $\mu=0$, and hence, $\mathcal{O}(\sqrt{\varepsilon})$ layers appear in the neighborhood of $x=0$ and $x=1$. For the second case, layer widths $\mathcal{O}(\varepsilon/\mu)$ and $\mathcal{O}(\mu)$ appear in the neighborhood of $x=0$ and $x=1$, respectively.

3. Bounds of Continuous Solution and Its Derivatives

Let us define a differential operator $\mathcal{L}_{\varepsilon,\mu}$ on the continuous solution $u(x,t)$ of problems (3) and (4) by

$$\begin{aligned}\mathcal{L}_{\varepsilon,\mu}(u(x,t)) \equiv{}& u_t(x,t) - \varepsilon u_{xx}(x,t) - \mu a(x,t)u_x(x,t)\\ &+ b(x,t)u(x,t).\end{aligned} \tag{6}$$

It is assumed that the data are compatible at its boundary and then the following compatibility conditions should satisfy at the corner points $(0,0)$, $(1,0)$, $(0,-\tau)$, and $(1,-\tau)$.

$$\begin{aligned} \gamma_b(0,0) &= \gamma_l(0), \\ \gamma_b(1,0) &= \gamma_r(0), \\ \mathscr{L}_{\varepsilon,\mu}(u(0,0)) &= c(0,0)u(0,-\tau) + f(0,0), \\ \mathscr{L}_{\varepsilon,\mu}(u(1,0)) &= c(1,0)u(1,-\tau) + f(1,0), \end{aligned} \tag{7}$$

which makes sense whenever $\gamma_l \in \mathscr{C}^1(\Gamma_l)$, $\gamma_r \in \mathscr{C}^1(\Gamma_r)$, and $\gamma_b \in \mathscr{C}^{2,1}(\Gamma_b)$. The uniqueness and existence of $u(x,t) \in \mathscr{C}^{2,1}(\overline{\mathscr{D}})$ are established depending on these conditions, and it is also necessary to show the differential operator, and $\mathscr{L}_{\varepsilon,\mu}$ satisfies the maximum principle.

Lemma 1. *Continuous maximum principle*

Suppose $\Psi(x,t) \in \mathscr{C}^{2,1}(\mathscr{D}) \cap \mathscr{C}^{0,0}(\overline{\mathscr{D}})$, such that $\Psi(x,t) \geq 0, \forall (x,t) \in \Gamma$ and $\mathscr{L}_{\varepsilon,\mu}[\Psi(x,t)] \geq 0, \forall (x,t) \in \mathscr{D}$. Then, $\Psi(x,t) \geq 0, \forall (x,t) \in \overline{\mathscr{D}}$.

Proof. Refer [34] □

Lemma 2. *The solution of equations (3) and (4) satisfies the following bounds:*

$$\begin{aligned} \left|u(x,t) - \gamma_b(x,0)\right| &\leq Ct, \\ \|u(x,t)\| &\leq C, \end{aligned} \tag{8}$$

for some constant C independent of ε and μ.

Proof. Set two barrier functions defined as

$$\begin{aligned} s(x,t) &= \begin{cases} u(x,t) - \gamma_b(x,0), & 0 \leq t \leq T, \\ u(x,t) - \gamma_b(x,t), & -\tau \leq t \leq 0, \end{cases} \\ q(x,t) &= \begin{cases} Ct, & 0 \leq t \leq T, \\ 0, & -\tau \leq t \leq 0, \end{cases} \end{aligned} \tag{9}$$

applying the differential operator

$$\begin{aligned} \mathscr{L}_{\varepsilon,\mu}[s(x,t)] &= \begin{cases} c(x,t)\gamma_b(x,t-\tau) + f(x,t) + \varepsilon \dfrac{d^2}{dx^2}\gamma_b(x,0) + \mu a \dfrac{d}{dx}\gamma_b(x,0) - b\gamma_b(x,0), & 0 \leq t \leq T, \\ 0, & -\tau \leq t \leq 0, \end{cases} \\ \mathscr{L}_{\varepsilon,\mu}[q(x,t)] &= \begin{cases} C(bt+1), & 0 \leq t \leq T, \\ 0, & -\tau \leq t \leq 0. \end{cases} \end{aligned} \tag{10}$$

For sufficiently large C, we have

$$\left|\mathscr{L}_{\varepsilon,\mu}[s(x,t)]\right| \leq \mathscr{L}_{\varepsilon,\mu}[q(x,t)]. \tag{11}$$

Since $\mathscr{L}_{\varepsilon,\mu}$ satisfies the maximum principle, it holds the comparison relation $|s(x,t)| \leq q(x,t)$. *i.e*, $|u(x,t) - \gamma_b(x,0)| \leq Ct$.

Using the relation $|u(x,t)| - |\gamma_b(x,0)| \leq |u(x,t) - \gamma_b(x,0)| \leq Ct$, as T is the maximum of t, $|u(x,t)| \leq Ct + |\gamma_b(x,0)| \leq CT + |\gamma_b(x,0)|$, then $|u(x,t)| \leq C$.

Taking the supreme of all $(x,t) \in \overline{\mathscr{D}}$, we arrive $\|u(x,t)\| \leq C$. □

Lemma 3. *For non-negative integers i and j, such that $0 \leq i + 2j \leq 4$, the derivatives of solution of problems (3) and (4) satisfy the following bounds:*

$$\left\|\frac{\partial^{i+j}u}{\partial x^i \partial t^j}\right\| \leq \begin{cases} C\varepsilon^{-(1/2)i}, & \alpha\mu^2 \leq \varsigma\varepsilon, \\ C\left(\dfrac{\mu}{\varepsilon}\right)^i \left(\dfrac{\mu^2}{\varepsilon}\right)^j, & \alpha\mu^2 \geq \varsigma\varepsilon, \end{cases} \text{, choosing } \varsigma = \min_{(x,t)\in\overline{\mathscr{D}}} \left\{\frac{b(x,t)}{a(x,t)}\right\}. \tag{12}$$

Proof (see [6]).

For the purpose of error analysis, it is necessary to decompose the solution $u(x,t)$ of problems (3) and (4) into a regular component $v(x,t)$, which characterizes the solution behavior outside the boundary layers, and a singular component $w(x,t)$, which characterizes the solution behavior inside the boundary layers. Further, we decompose the singular component into the sum of left and right singular parts $w(x,t) = w_L(x,t) + w_R(x,t)$ such that $u(x,t) = v(x,t) + w_L(x,t) + w_R(x,t)$. The components individually satisfy

$$\begin{cases} \mathscr{L}_{\varepsilon,\mu}(v) = c(x,t)v(x,t-\tau) + f(x,t), \\ v(x,t) = u(x,t), \text{on } \Gamma_b, \\ v(0,t) = \varphi_{ol}(t), \text{(conveniently chosen)}, \\ v(1,t) = \varphi_{or}(t), \text{(conveniently chosen)}, \end{cases} \tag{13}$$

$$\begin{cases} \mathscr{L}_{\varepsilon,\mu}(w_L) = c(x,t)w_L(x,t-\tau), \\ w_L(x,t) = 0, \text{on } \Gamma_b, \\ w_L(1,t) = 0, \\ w_L(0,t) = u(0,t) - v(0,t), \end{cases} \tag{14}$$

$$\begin{cases} \mathscr{L}_{\varepsilon,\mu}(w_R) = c(x,t)w_R(x,t-\tau), \\ w_R(x,t) = 0, \text{on } \Gamma_b, \\ w_R(0,t) = 0, \\ w_R(1,t) = u(1,t) - v(1,t). \end{cases} \tag{15}$$

Some prior bounds of the components of the continuous solution and their derivatives are given in the following lemmas, which are necessary for the later error estimate. □

Lemma 4. *The bounds of the left and right singular components have given by*

$$\begin{aligned} |w_L| &\le \begin{cases} C\exp\left(-\dfrac{\sqrt{\alpha\varsigma}}{\sqrt{\varepsilon}}\,x\right), & \alpha\mu^2 \le \varsigma\varepsilon, \\ C\exp\left(-\dfrac{\alpha\mu}{\varepsilon}x\right), & \alpha\mu^2 \ge \varsigma\varepsilon, \end{cases} \\ |\mathrm{w_R}| &\le \begin{cases} C\exp\left(-\dfrac{\sqrt{\alpha\varsigma}}{2\sqrt{\varepsilon}}(1-\mathrm{x})\right), & \alpha\mu^2 \le \varsigma\varepsilon, \\ C\exp\left(-\dfrac{\varsigma}{2\mu}(1-\mathrm{x})\right), & \alpha\mu^2 \ge \varsigma\varepsilon. \end{cases} \end{aligned} \tag{16}$$

Proof (see [6]). □

Lemma 5. *The derivatives of regular and singular components of $u(x,t)$ satisfy the following bounds:*

(i) If $\alpha\mu^2 \ge \varsigma\varepsilon$, then

$$\begin{aligned} &\left\|\frac{\partial^{i+j}v}{\partial x^i \partial t^j}\right\| \le C\left(1 + \left(\frac{\varepsilon}{\mu}\right)^{3-i}\left(\frac{\mu^2}{\varepsilon}\right)^j\right), \quad \text{for } 0 \le i + 2j \le 4, \\ &\left\|\frac{\partial^i w_L}{\partial x^i}\right\| \le C\left(\frac{\mu}{\varepsilon}\right)^i, \quad \text{for } 0 \le i \le 4, \\ &\left\|\frac{\partial^2 w_L}{\partial \mathrm{t}^2}\right\| \le C\left(1 + \mu^2\varepsilon^{-1}\right), \\ &\left\|\frac{\partial^i w_R}{\partial x^i}\right\| \le C\left(\mu^{-i} + \mu^{-1}\varepsilon^{2-i}\right), \quad \text{for } 0 \le i \le 4, \\ &\left\|\frac{\partial^j w_R}{\partial t^j}\right\| \le C \quad \text{for } j = 1, 2. \end{aligned} \tag{17}$$

(ii) If $\alpha\mu^2 \le \varsigma\varepsilon$, then

$$\left\|\frac{\partial^{i+j}v}{\partial x^i \partial t^j}\right\| \le C, \quad \text{for } 0 \le i + 2j \le 4. \tag{18}$$

The derivative bounds of w_L and w_R satisfy the derivative bounds of u (x, t) under Lemma 3.

Proof. Refer [32]. □

4. Formulation of Numerical Scheme

Applying the Crank–Nicolson approach upon uniform discretization for time and using midpoint central finite difference approximation on Shishkin mesh type in spatial direction, the derivation is explained in the following subsections.

4.1. Semidiscretization. The temporal discretization is performed by uniform mesh extending up to the time-lag interval as

$$\begin{aligned} \mathscr{D}_t^M &= \{t_j = j\Delta t, j = 0, 1, \ldots, M\}, \\ \mathscr{D}_t^m &= \{t_j = j\Delta t, j = -1, -2, \ldots, -(m+1)\}, \end{aligned} \tag{19}$$

where M and m are the number of meshes in the intervals $[0, T]$ and $[-\tau, 0]$, respectively, assuming that M is a positive multiple of m.

For problems (3) and (4) at $(x, t_{j+(1/2)})$, the mean point of (x, t_j) and (x, t_{j+1}), for all $x \in \overline{\mathscr{D}}_x$, is given by

$$\begin{aligned} &\left(-\varepsilon\frac{\partial^2 u}{\partial x^2} - \mu a\left(x, t_{j+(1/2)}\right)\frac{\partial u}{\partial x} + b\left(x, t_{j+(1/2)}\right)u + \frac{\partial u}{\partial t}\right)\left(x, t_{j+(1/2)}\right) \\ &\quad = -c\left(x, t_{j+(1/2)}\right)u\left(x, t_{j+(1/2)-m}\right) + f\left(x, t_{j+(1/2)}\right). \end{aligned} \tag{20}$$

Applying Taylor's series expansion of (x, t_j) and (x, t_{j+1}) about $(x, t_{j+(1/2)})$, we have

$$\begin{aligned} u(x, t+\Delta t) &= u\left(x, t + \frac{1}{2}\Delta t\right) + \frac{\Delta t}{2}\frac{\partial}{\partial t}u\left(x, t + \frac{1}{2}\Delta t\right) \\ &\quad + \frac{1}{2}\left(\frac{\Delta t}{2}\right)^2\frac{\partial^2}{\partial t^2}u\left(x, t + \frac{1}{2}\Delta t\right) + \ldots, \\ u(x, t) &= u\left(x, t + \frac{1}{2}\Delta t\right) - \frac{\Delta t}{2}\frac{\partial}{\partial t}u\left(x, t + \frac{1}{2}\Delta t\right) \\ &\quad + \frac{1}{2}\left(\frac{\Delta t}{2}\right)^2\frac{\partial^2}{\partial t^2}u\left(x, t + \frac{1}{2}\Delta t\right) - + \ldots. \end{aligned} \tag{21}$$

From these expansions, we can derive

$$\frac{\partial}{\partial t}u\left(x, t + \frac{1}{2}\Delta t\right) = \frac{u(x, t+\Delta t) - u(x, t)}{\Delta t} + \mathscr{O}\left((\Delta t)^2\right). \tag{22}$$

At $(p+1)^{st}$ time step, we substitute (22) for time derivative and average values between (x, t_p) and (x, t_{P+1}) for spatial derivatives into (20) and we obtain

$$\left[2\mathscr{I} + \Delta t \mathscr{L}_{\varepsilon,\mu}^{M}\right] u\left(x, t_{p+1}\right) = g\left(x, t_{p+1}\right), \tag{23}$$

where $\mathscr{I}$ is the identity differential operator, $\mathscr{L}_{\varepsilon,\mu}^{M} \equiv -\varepsilon(d^2/dx^2) - \mu a(x, t_{p+(1/2)})(d/dx) + b(x, t_{p+(1/2)})$, and $g(x, t_{p+1}) = [2\mathscr{I} - \Delta t \mathscr{L}_{\varepsilon,\mu}^{M}] u(x, t_p) - \Delta t c(x, t_{p+(1/2)})[u(x, t_{p+1-m}) + u(x, t_{p-m})] + 2\Delta t f(x, t_{p+(1/2)})$ that possess a truncation error of $\mathscr{O}((\Delta t)^3)$.

Equation (23) gives the semidiscrete boundary value problem formulation of problems (3) and (4) for each time step t_{p+1} with the boundary conditions as

$$\begin{cases} u\left(0, t_{p+1}\right) = \gamma_l\left(t_{p+1}\right), \\ u\left(1, t_{p+1}\right) = \gamma_r\left(t_{p+1}\right), \end{cases} \tag{24}$$
$$u\left(x, t_{p+1-m}\right) = \gamma_b\left(x, t_{p+1-m}\right), \text{when } p \le m-1.$$

Let $\overline{u}^j(x)$ be the numerical solution of the semidiscrete problem whose exact solution is $u(x, t_j)$ at a fixed $t = t_j$ and $\mathscr{L}_{\varepsilon,\mu}^{M}(u(x, t_{j-1}) - \overline{u}^j(x))$ is the truncation error caused by one step of iteration which is called local truncation error. Hence, the jth local absolute maximum error $|e_j| = |u(x, t_{j-1}) - \overline{u}^j(x)| \le C(\Delta t)^3$. The global truncation error TE_j is the cumulative truncation error up to j^{th} iteration. Let E determine E_M (the global error throughout the whole time interval).

Lemma 6. *The global error estimate, E of the semidiscrete problem (23) and (24), is given by*

$$\|E\| \le C(\Delta t)^2. \tag{25}$$

Proof. The jth local maximum absolute error, e_j, is bounded by

$$\begin{aligned} \left|e_j\right| &\le C(\Delta t)^3, \\ E &= \sum_{j=1}^{M} e_j, \text{ then} \\ |E| &= \left|\sum_{j=1}^{M} e_j\right| \le \sum_{j=1}^{M} \left|e_j\right| \le \sum_{j=1}^{M} \left|C(\Delta t)^3\right| \\ &= \mathrm{CM}(\Delta t)^3 = \mathrm{CT}(\Delta t)^2 = C(\Delta t)^2. \end{aligned} \tag{26}$$

Thus, $\|E\| \le C(\Delta t)^2$.

Considering the semidiscretization, at each time step p, the differential operator $[2\mathscr{I} + \Delta t \mathscr{L}_{\varepsilon,\mu}^{M}]$, defined in 23 satisfies the maximum principle. □

Lemma 7. *Semidiscrete maximum principle*

For a fixed time $t = t_{p+1}$, let the function $\Psi(x, t_{p+1}) \in \mathscr{C}^2(0,1)$, satisfies $\Psi(0, t_{p+1}), \Psi(1, t_{p+1}) \ge 0$, and $[2\mathscr{I} + \mathscr{L}_{\varepsilon,\mu}^{M}](\Psi(x, t_{p+1})) \ge 0, \forall x \in (0,1)$. Then, $\Psi(x, t_{p+1}) \ge 0, \forall x \in [0,1]$.

Proof. We apply a similar technique of contradiction as the continuous maximum principle of Lemma 1.

Let $(x', t_{p+1}) \in \overline{D}$ as $\Psi(x', t_{p+1}) = \min_{(x, t_{p+1}) \in \overline{D}} \{\Psi(x, t_{p+1})\}$. Supposition of $\Psi(x', t_{p+1}) < 0$ implies a contradiction of the given hypothesis and hence proved. □

Lemma 8. *Semidiscretization uniform stability*

The solution $u(x, t_{p+1})$ of equations (23) and (24) satisfies

$$\left\|u\left(x, t_{p+1}\right)\right\| \le \frac{1}{\Delta t \beta}\|g\| + \max_x\left\{\left|\gamma_l\left(0, t_{p+1}\right)\right|, \left|\gamma_r\left(1, t_{p+1}\right)\right|\right\}. \tag{27}$$

Proof. Define barrier functions

$$\theta^{\pm}\left(x, t_{p+1}\right) = \frac{1}{\Delta t \beta}\|g\| + \max_x\left\{\left|\gamma_l\left(0, t_{p+1}\right)\right|, \left|\gamma_r\left(1, t_{p+1}\right)\right|\right\} \pm u\left(x, t_{p+1}\right). \tag{28}$$

We have

$$\begin{aligned} \theta^{\pm}\left(0, t_{p+1}\right) &= \frac{1}{\Delta t \beta}\|g\| + \max_x\left\{\left|\gamma_l\left(0, t_{p+1}\right)\right|, \left|\gamma_r\left(1, t_{p+1}\right)\right|\right\} \pm \gamma_l\left(0, t_{p+1}\right) \ge 0, \\ \theta^{\pm}\left(1, t_{p+1}\right) &= \frac{1}{\Delta t \beta}\|g\| + \max_x\left\{\left|\gamma_l\left(0, t_{p+1}\right)\right|, \left|\gamma_r\left(1, t_{p+1}\right)\right|\right\} \pm \gamma_r\left(1, t_{p+1}\right) \ge 0, \\ \left[2\mathscr{I} + \Delta t \mathscr{L}_{\varepsilon,\mu}^{M}\right]\left(\theta^{\pm}\left(x, t_{p+1}\right)\right) &= \pm\left[2\mathscr{I} + \Delta t \mathscr{L}_{\varepsilon,\mu}^{M}\right] u\left(x, t_{p+1}\right) + (2 + b\Delta t)\left(\frac{1}{\Delta t \beta}\|g\| + \max_x\left\{\left|\gamma_l\left(0, t_{p+1}\right)\right|, \left|\gamma_r\left(1, t_{p+1}\right)\right|\right\}\right) \\ &= \pm g\left(x, t_{p+1}\right) + \frac{b}{\beta}\|g\| + \frac{2}{\Delta t \beta}\|g\| + (2 + b\Delta t)\left(\max_x\left\{\left|\gamma_l\left(0, t_{p+1}\right)\right|, \left|\gamma_r\left(1, t_{p+1}\right)\right|\right\}\right) \\ &\ge 0. \end{aligned} \tag{29}$$

Thus, applying Lemma 7 gives the required result.

The boundary layer properties are determined according to the characteristic equation of (23), which is

$$-\varepsilon(\lambda(x))^2 - \mu a\lambda(x) + \left(b + \frac{2}{\Delta t}\right) = 0, \tag{30}$$

whose roots are

$$\begin{aligned} \lambda_1(x) &= -\frac{\mu a}{2\varepsilon}\left[1 + \sqrt{1 + \frac{4\varepsilon}{\mu^2 a^2}\left(b + \frac{2}{\Delta t}\right)}\right], \\ \lambda_2(x) &= -\frac{\mu a}{2\varepsilon}\left[1 - \sqrt{1 + \frac{4\varepsilon}{\mu^2 a^2}\left(b + \frac{2}{\Delta t}\right)}\right]. \end{aligned} \tag{31}$$

Let

$$\begin{aligned} \Lambda_1 &= -\max_x\{\lambda_1(x)\}, \\ \Lambda_2 &= \min_x\{\lambda_2(x)\}. \end{aligned} \tag{32}$$

□

Lemma 9. *The bound of the solution, $u(x, t_{p+1})$ of the discrete problem (23) and (24), is provided by*

$$\begin{aligned} &\left|\frac{d^i}{dx^i}u\left(x, t_{p+1}\right)\right| \\ &\quad \le C\left[1 + \Lambda_1^i \exp(-\rho\Lambda_1 x) + \Lambda_2^i \exp(-\rho\Lambda_2(1-x))\right], \end{aligned} \tag{33}$$

up to a certain prescribed order q, for $0 \le i \le q$ and $0 < \rho < 1$.

Proof. Refer [5, 35]. □

4.2. Full Discretization. Depending on the prior knowledge of boundary layers' width and position, we apply piece-wise uniform Shishkin mesh type for spatial discretization. Let the transition points be σ_1 and σ_2. Then, divide the spatial domain component $[0, 1]$ into three subintervals $[0, \sigma_1]$, $[\sigma_1, 1-\sigma_2]$, and $[1-\sigma_2, 1]$. According to Shishkin mesh [36], each subinterval $[0, \sigma_1]$, $[\sigma_1, 1-\sigma_2]$ and $[1-\sigma_2, 1]$ will be divided into a uniform mesh size of $(N/4)$, $(N/2)$ and $(N/4)$, respectively, where N is the number of meshes in spatial direction assuming that it is a multiple of 4. The transition points σ_1 and σ_2 are determined by

$$\begin{aligned} \sigma_1 &= \begin{cases} \min\left\{\frac{1}{4}, \frac{4\sqrt{\varepsilon}}{\sqrt{\varsigma\alpha}}\ln N\right\}, & \mu^2 \le \frac{\varsigma\varepsilon}{\alpha}, \\ \min\left\{\frac{1}{4}, \frac{4\varepsilon}{\mu\alpha}\ln N\right\}, & \mu^2 \ge \frac{\varsigma\varepsilon}{\alpha}, \end{cases} \\ \sigma_2 &= \begin{cases} \min\left\{\frac{1}{4}, \frac{8\sqrt{\varepsilon}}{\sqrt{\varsigma\alpha}}\ln N\right\}, & \mu^2 \le \frac{\varsigma\varepsilon}{\alpha}, \\ \min\left\{\frac{1}{4}, \frac{8\mu}{\varsigma}\ln N\right\}, & \mu^2 \ge \frac{\varsigma\varepsilon}{\alpha}. \end{cases} \end{aligned} \tag{34}$$

So, the spatial discretization, $\mathscr{D} = \{0 = x_1, x_2, \ldots, x_{N/4} = \sigma_1, \ldots, x_{3N/4} = 1-\sigma_2, \ldots, x_{N+1} = 1\}$, where

$$x_i = \begin{cases} \frac{4}{N}\sigma_1(i-1), & i = 1, 2, \ldots, \frac{N}{4}+1, \\ \sigma_1 + \frac{2}{N}(1-\sigma_1-\sigma_2)\left(i - 1 - \frac{N}{4}\right), & i = \frac{N}{4}+1, \ldots, \frac{3N}{4}+1, \\ 1 - \sigma_2 + \frac{4}{N}\sigma_2\left(i - 1 - \frac{3N}{4}\right), & i = \frac{3N}{4}+1, \ldots, N+1. \end{cases} \tag{35}$$

Extending the semidiscretized equation (23) to full discretization using central difference approximation for a fixed time $t = t_p$, since the spatial discretization is non-uniform mesh, we have the finite difference approximations, $(d^2/dx^2)u(x_i, t_p) \approx \delta_x^2 u_{i,p} = (2/h_i + h_{i+1})\ ((u_{i+1,p} - u_{i,p}/h_{i+1}) - (u_{i,p} - u_{i-1,p}/h_i))$ and $(d/dx)u(x_i, t_p) \approx \delta_x^o u_{i,p} = (u_{i+1,p} - u_{i-1,p}/h_i + h_{i+1})$ for each mesh point (x_i, t_p). Note that $u_{i,j} = u(x_i, t_j)$. Then, the finite difference scheme of equations (23) and (24) becomes

$$\begin{aligned} &\frac{u_{i,j+1} - u_{i,j}}{\Delta t} - \varepsilon\frac{1}{2}\left(\delta_x^2 u_{i,j+1} + \delta_x^2 u_{i,j}\right) - \mu\frac{1}{2}a_{i,j+(1/2)}\left(\delta_x^o u_{i,j+1} + \delta_x^o u_{i,j}\right) + \frac{1}{2}b_{i,j+(1/2)}\left(u_{i,j+1} + u_{i,j}\right) \\ &\quad = \frac{1}{2}c_{i,j+(1/2)}\left(u_{i,j+1-m} + u_{i,j-m}\right) + f_{i,j+(1/2)}, \end{aligned} \tag{36}$$

or equivalently, using the Crank–Nicolson finite difference formula,

$$\delta_t^o u_{i,j+(1/2)} - \varepsilon\delta_x^2 u_{i,j+(1/2)} - \mu a_{i,j+(1/2)}\delta_x^o u_{i,j+(1/2)} + b_{i,j+(1/2)}u_{i,j+(1/2)} = \frac{1}{2}c_{i,j+(1/2)}\left(u_{i,j+1-m} + u_{i,j-m}\right) + f_{i,j+(1/2)}, \tag{37}$$

for all $i = 1, 2, \ldots, N+1$ and $j = 1, 2, \ldots, M+1$.

Defining a difference operator $\mathscr{L}_{\varepsilon,\mu}^{M,N} = \delta_t^o - \varepsilon\delta_x^2 - \mu a_{i,j+(1/2)}\delta_x^o + b_{i,j+(1/2)}$, the corresponding difference equation can be written as

$$\left[\mathscr{L}_{\varepsilon,\mu}^{M,N}\right]\left(u_{i,j+(1/2)}\right) = \frac{1}{2}c_{i,j+(1/2)}\left(u_{i,j+1-m} + u_{i,j-m}\right) + f_{i,j+(1/2)}, \tag{38}$$

which is

$$\begin{aligned} &2u_{i,j+1} + \Delta t\left\{-\varepsilon\left[\frac{2}{h_i + h_{i+1}}\left(\frac{u_{i+1,j+1} - u_{i,j+1}}{h_{i+1}} - \frac{u_{i,j+1} - u_{i-1,j+1}}{h_i}\right)\right] - \mu a_{i,j+(1/2)}\left[\frac{u_{i+1,j+1} - u_{i-1,j+1}}{h_i + h_{i+1}}\right] + b_{i,j+(1/2)}u_{i,j+1}\right\} \\ &= 2u_{i,j} - \Delta t\left\{-\varepsilon\left[\frac{2}{h_i + h_{i+1}}\left(\frac{u_{i+1,j} - u_{i,j}}{h_{i+1}} - \frac{u_{i,j} - u_{i-1,j}}{h_i}\right)\right] - \mu a_{i,j+(1/2)}\left[\frac{u_{i+1,j} - u_{i-1,j}}{h_i + h_{i+1}}\right] + b_{i,j+(1/2)}u_{i,j}\right\} \\ &\quad + \Delta t c_{i,j+(1/2)}\left(u_{i,j+1-m} + u_{i,j-m}\right) + 2\Delta t f_{i,j+(1/2)}. \end{aligned} \tag{39}$$

Taking all terms with unknown nodal values to the left and known values to the right, it has a recurrence form of

$$\begin{aligned} &\left(-\frac{2\varepsilon\Delta t}{h_i(h_i + h_{i+1})} + \frac{\mu a_{i,j+(1/2)}\Delta t}{h_i + h_{i+1}}\right)u_{i-1,j+1} + \left(\frac{2\varepsilon\Delta t}{h_{i+1}(h_i + h_{i+1})} + \frac{2\varepsilon\Delta t}{h_i(h_i + h_{i+1})} + \Delta t b_{i,j+(1/2)} + 2\right)u_{i,j+1} \\ &\quad + \left(-\frac{2\varepsilon\Delta t}{h_{i+1}(h_i + h_{i+1})} - \frac{\mu a_{i,j+(1/2)}\Delta t}{h_i + h_{i+1}}\right)u_{i+1,j+1} \\ &= \left(\frac{2\varepsilon\Delta t}{h_i(h_i + h_{i+1})} - \frac{\mu a_{i,j+(1/2)}\Delta t}{h_i + h_{i+1}}\right)u_{i-1,j} + \left(-\frac{2\varepsilon\Delta t}{h_{i+1}(h_i + h_{i+1})} - \frac{2\varepsilon\Delta t}{h_i(h_i + h_{i+1})} - \Delta t b_{i,j+(1/2)} + 2\right)u_{i,j} \\ &\quad + \left(\frac{2\varepsilon\Delta t}{h_{i+1}(h_i + h_{i+1})} + \frac{\mu a_{i,j+(1/2)}\Delta t}{h_i + h_{i+1}}\right)u_{i+1,j} + \Delta t c_{i,j+(1/2)}\left(u_{i,j+1-m} + u_{i,j-m}\right) + 2\Delta t f_{i,j+(1/2)}. \end{aligned} \tag{40}$$

For each time step $(j+1)$, for all $i = 2, \cdots, N$, we drive an $(N-1)\times(N-1)$ tridiagonal system of equation,

$$(A_i^-)u_{i-1,j+1} + (A_i^o + 2)u_{i,j+1} + (A_i^+)u_{i+1,j+1} = g_{i,j+1}, \tag{41}$$

given all the discrete initial and boundary values

$$\begin{aligned} u_{i,j} &= \gamma_b\left(x_i, t_j\right), \quad \forall i, \text{and } j = -m, -m+1, \cdots, 0 \\ u_{1,j} &= \gamma_l\left(t_j\right), \quad \forall j, \\ u_{N+1,j} &= \gamma_r\left(t_j\right), \quad \forall j, \end{aligned} \tag{42}$$

where

$$\begin{aligned} A_i^- &= -\frac{2\varepsilon\Delta t}{h_i(h_i + h_{i+1})} + \frac{\mu a_{i,j+(1/2)}\Delta t}{h_i + h_{i+1}}, \\ A_i^+ &= -\frac{2\varepsilon\Delta t}{h_{i+1}(h_i + h_{i+1})} - \frac{\mu a_{i,j+(1/2)}\Delta t}{h_i + h_{i+1}}, \\ A_i^o &= \frac{2\varepsilon\Delta t}{h_{i+1}(h_i + h_{i+1})} + \frac{2\varepsilon\Delta t}{h_i(h_i + h_{i+1})} + \Delta t b_{i,j+(1/2)}, \\ g_{i,j+1} &= (-A_i^-)u_{i-1,j} + (-A_i^o + 2)u_{i,j} + (-A_i^+)u_{i+1,j} \\ &\quad + \Delta t c_{i,j+(1/2)}\left(u_{i,j+1-m} + u_{i,j-m}\right) + 2\Delta t f_{i,j+(1/2)}. \end{aligned} \tag{43}$$

5. Convergence of Numerical Method

Lemma 10. *If a square matrix $A = [a_{i,j}]$ is real, irreducible, diagonally dominant with $a_{i,j} \le 0$, and $a_{i,i} > 0$ for all i and j, then $A^{-1} > \mathbf{0}$, where $\mathbf{0}$ is a zero matrix.*

Proof (see[37]).

This lemma can be a useful tool for establishing the conditions under which the scheme's coefficient matrix has an inverse. Let us examine each hypothesis in turn.

(i) The coefficient matrix of the system (41) is real,

(ii) As $A_i^o = (2\varepsilon\Delta t/h_{i+1}(h_i + h_{i+1})) + (2\varepsilon\Delta t/h_i(h_i + h_{i+1})) + \Delta t b_{i,j+(1/2)} > 0$, all diagonal entries are positive,

(iii) Under the assumption of $\|a\|\mu h < 2\varepsilon$, for coarse mesh size h, the lower and upper diagonal entries, $A_i^- = -(2\varepsilon\Delta t/h_i(h_i + h_{i+1})) + (\mu a_{i,j+(1/2)}\Delta t/h_i + h_{i+1}) < 0$ and $A_i^+ = -(2\varepsilon\Delta t/h_{i+1}(h_i + h_{i+1})) - (\mu a_{i,j+(1/2)}\Delta t/h_i + h_{i+1}) < 0$. Then, all off-diagonal entries of the coefficient matrix are nonpositive,

(iv) $|A_i^-| = (2\varepsilon\Delta t/h_i(h_i + h_{i+1})) - (\mu a_{i,j+(1/2)}\Delta t/h_i + h_{i+1})$ and $|A_i^+| = (2\varepsilon\Delta t/h_{i+1}(h_i + h_{i+1})) + (\mu a_{i,j+(1/2)}\Delta t/h_i + h_{i+1})$, which implies $|A_i^o| \ge |A_i^-| + |A_i^+|$. Since all the rest entries in i^{th} row are zero, the matrix is diagonally dominant

(v) The irreducibility of the matrix can be shown using directed graph analysis. If the directed graph of a matrix is strongly connected, then it is irreducible. One can refer [37] for more about the directed graph. For the positional i^{th} nonzero entry $\mathbf{P}_i$, inhibiting the self-mapping of the diagonal entries, the directed graph of the tridiagonal coefficient matrix resembles Figure 1, which is strongly connected, and hence, the coefficient matrix is irreducible.

The descriptions i through v satisfy all the hypotheses of Lemma 10, and then the coefficient matrix is invertible, and we guarantee to determine the numerical solution uniquely. These properties are also verification of the matrix A being an M-matrix, which is a monotone matrix. The monotonicity of a matrix establishes the discrete maximum principle. □

Lemma 11. *Discrete maximum principle*

Given a discrete function, $\varphi_{i,j}$ with $\varphi_{1,j}, \varphi_{N+1,j} \ge 0, \forall j = m+1, \ldots, m+M+1$ and $\varphi_{i,j} \ge 0, \forall i = 1, \ldots, N+1$ and $\forall j = 1, \ldots, m$. If $\mathscr{L}_{\varepsilon,\mu}^{M,N}(\varphi_{i,j}) \ge 0, \forall i = 2, \ldots, N$ and $\forall j = m+1, \ldots, m+M+1$, then $\varphi_{i,j} \ge 0, \forall i = 1, \ldots, N+1$ and $\forall j = m, \ldots, m+M+1$.

Remark 12. It is also necessary to investigate the assumption $\|a\|\mu h < 2\varepsilon$ for the two major cases $\alpha\mu^2 \le \varsigma\varepsilon$ and $\alpha\mu^2 \ge \varsigma\varepsilon$. In both cases, h is greater than or equal to $1/N$. This comparison with the assumption implies $(1/N) \le (2\epsilon/\alpha\mu)$ which is

$$\frac{\mu^2}{\varepsilon} \le \frac{\varsigma}{\alpha}\left(\frac{2N}{\varsigma}\right). \tag{44}$$

Considering the first case, $\alpha\mu^2 \le \varsigma\varepsilon$, there exist N_o such that the assumption (44) holds for all $N \ge N_o$. More generally, when $(\mu^2/\varepsilon) \longrightarrow 0$ as $\varepsilon \longrightarrow 0$, the system (41) converges for all $N \ge N_o$ for some positive integer N_o. But for the other case $\alpha\mu^2 \ge \varsigma\varepsilon$, the assumption 34 holds for some fortunate large N. That is, when $(\varepsilon/\mu^2) \longrightarrow 0$ as $\mu \longrightarrow 0$, the system does not converge.

5.1. Error Bounds. Alike the continuous solution decomposed into regular and singular components in Section 3, $(u = v + w_L + w_R)$, the numerical solution can be also decomposed as $U = V + W_L + W_R$, with a similar property, which is discretely defined as

$$\begin{cases} \left(\mathscr{L}_{\varepsilon,\mu}^{M,N}\right)\left(V_{i,j+(1/2)}\right) = \dfrac{1}{2}c_{i,j+(1/2)}\left(V_{i,j+1-m} + V_{i,j-m}\right) + f_{i,j+(1/2)}, & \text{on } \mathscr{D}^{N\times M}, \\ V_{i,j+(1/2)} = v_{i,j+(1/2)}, & \text{on } \Gamma^{N\times M}, \end{cases} \tag{45}$$

$$\begin{cases} \left(\mathscr{L}_{\varepsilon,\mu}^{M,N}\right)\left(W_{L:i,j+(1/2)}\right) = \dfrac{1}{2}c_{i,j+(1/2)}\left(W_{L:i,j+1-m} + W_{L:i,j-m}\right), & \text{on } \mathscr{D}^{N\times M}, \\ W_{L:i,j+(1/2)} = w_{L:i,j+(1/2)}, & \text{on } \Gamma^{N\times M}, \end{cases} \tag{46}$$

$$\begin{cases} \left(\mathscr{L}_{\varepsilon,\mu}^{M,N}\right)\left(W_{R:i,j+(1/2)}\right) = \dfrac{1}{2}c_{i,j+(1/2)}\left(W_{R:i,j+1-m} + W_{R:i,j-m}\right), & \text{on } \mathscr{D}^{N\times M}, \\ W_{R:i,j+(1/2)} = w_{R:i,j+(1/2)}, & \text{on } \Gamma^{N\times M}, \end{cases} \tag{47}$$

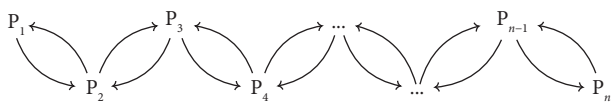

Figure 1: The directed graph of the coefficient matrix.

then the error

$$U - u = (V - v) + (W_L - w_L) + (W_R - w_R). \tag{48}$$

The triangle inequality law gives its bound with

$$\|U - u\| \le \|V - v\| + \|W_L - w_L\| + \|W_R - w_R\|. \tag{49}$$

As we discuss in Section 2, the numerical solution is intended to compute in the time step of τ one after the other. So, the error analysis is performed in two intervals of time, when $0 < j < m$ or $t \in [0, \tau]$, and $m + 1 \le j \le M + 1$ or $t \in [\tau, T]$.

Case I: When $t \in [0, \tau]$

The source function, $(f(x,t))$ in the right-hand side, the retarded term as well, is a known function. For this case, the analysis is computed as a nondelay differential equation.

Lemma 13. *The singular components of the discrete solution satisfy*

$$\begin{aligned} \left|(W_L)_{i,j+1/2}\right| &\le \mathrm{CN}^{-2}, \quad i = \frac{N}{4} + 1, \ldots, N + 1, \\ \left|(W_R)_{i,j+1/2}\right| &\le \mathrm{CN}^{-2}, \quad i = 1, \ldots, \frac{3N}{4} + 1. \end{aligned} \tag{50}$$

Proof. (see [32]).

The evaluation of the error estimate of each component starts with the truncation error of the components separately. The continuous regular component satisfies the continuous problem (13), and the discrete regular component satisfies the discrete problem (45). From differential equation (6) and difference equation (38), we have

$$\begin{aligned} \left[\mathscr{L}_{\varepsilon,\mu}^{M,N}\right](V - v)_{i,j+(1/2)} &= \left[\mathscr{L}_{\varepsilon,\mu}^{M,N}\right]V_{i,j+(1/2)} - \left[\mathscr{L}_{\varepsilon,\mu}^{M,N}\right]v_{i,j+(1/2)} \\ &= \left[\mathscr{L}_{\varepsilon,\mu}\right]v_{i,j+(1/2)} - \left[\mathscr{L}_{\varepsilon,\mu}^{M,N}\right]v_{i,j+(1/2)} \\ &= \left[\frac{\partial}{\partial t} - \delta_t^o\right]v_{i,j+(1/2)} - \varepsilon\left[\frac{\partial^2}{\partial x^2} - \delta_x^2\right]v_{i,j+(1/2)} - \mu a\left[\frac{\partial}{\partial x} - \delta_x^o\right]v_{i,j+(1/2)}. \end{aligned} \tag{51}$$

Hence, the truncation bound of the regular component is

$$\left\|\mathscr{L}_{\varepsilon,\mu}^{M,N}\left((V - v)_{i,j+(1/2)}\right)\right\| \le C\left(\Delta t^2 + \varepsilon(h_i + h_{i+1})^2\|v_{xxxx}\| + \mu(h_i + h_{i+1})^2\|v_{xxx}\|\right). \tag{52}$$

Similarly, the singular components satisfy the continuous problem (14) and (15) and discrete problem (46) and (47). Then, we derive

$$\left\|\mathscr{L}_{\varepsilon,\mu}^{M,N}\left((W_L - w_L)_{i,j+(1/2)}\right)\right\| \le C\left(\Delta t^2 + \varepsilon(h_i + h_{i+1})^2\|w_{Lxxxx}\| + \mu(h_i + h_{i+1})^2\|w_{Lxxx}\|\right), \tag{53}$$

and

$$\left\|\mathscr{L}_{\varepsilon,\mu}^{M,N}\left((W_R - w_R)_{i,j+(1/2)}\right)\right\| \le C\left(\Delta t^2 + \varepsilon(h_i + h_{i+1})^2\|w_{Rxxxx}\| + \mu(h_i + h_{i+1})^2\|w_{Rxxx}\|\right). \tag{54}$$

Lemma 14. *The left layer component satisfies the following error bound estimate:*

$$\|(W_L - w_L)\| \le \begin{cases} C\left[M^{-2} + N^{-2}(\ln N)^2\right], & \alpha\mu^2 \le \varsigma\varepsilon, \\ C\left[M^{-2} + N^{-2}(\ln N)^3\right], & \alpha\mu^2 \ge \varsigma\varepsilon. \end{cases} \tag{55}$$

Proof. In the left boundary layer region, $[0, \sigma_1]$, $h_i \le C.\sqrt{\varepsilon}N^{-1}\ln N$, if $\alpha\mu^2 \le \varsigma\varepsilon$ and $h_i \le C(\varepsilon/\mu)N^{-1}\ln N$, if $\alpha\mu^2 \ge \varsigma\varepsilon$. Applying the derivative bounds, equation (??) of Lemma 5, the bound of equation (53) gives

$$\begin{aligned} \left\|\mathscr{L}_{\varepsilon,\mu}^{M,N}(W_L - w_L)\right\| &\le \begin{cases} C\left[M^{-2} + \varepsilon\left(\sqrt{\varepsilon}\,N^{-1}\ln N\right)^2\left(\varepsilon^{-2}\right) + \mu\left(\sqrt{\varepsilon}\,N^{-1}\ln N\right)^2(\varepsilon)^{-(3/2)}\right], & \alpha\mu^2 \le \varsigma\varepsilon, \\ C\left[M^{-2} + \varepsilon\left(\frac{\varepsilon}{\mu}N^{-1}\ln N\right)^2\left(\mu^4\varepsilon^{-4}\right) + \mu\left(\frac{\varepsilon}{\mu}N^{-1}\ln N\right)^2\left(\mu^3\varepsilon^{-3}\right)\right], & \alpha\mu^2 \ge \varsigma\varepsilon, \end{cases} \\ &\le \begin{cases} C\left[M^{-2} + N^{-2}(\ln N)^2\left(1 + \frac{\mu}{\sqrt{\varepsilon}}\right)\right], & \alpha\mu^2 \le \varsigma\varepsilon, \\ C\left[M^{-2} + N^{-2}(\ln N)^2\left(\mu^2\varepsilon^{-1}\right)\right], & \alpha\mu^2 \ge \varsigma\varepsilon. \end{cases} \end{aligned} \tag{56}$$

Considering $(\mu/\sqrt{\varepsilon}) \le C$, when $\alpha\mu^2 \le \varsigma\varepsilon$ and $(\mu/\varepsilon) \le C\ln N$, when $\alpha\mu^2 \ge \varsigma\varepsilon$, we arrive

$$\left\|\mathscr{L}_{\varepsilon,\mu}^{M,N}(W_L - w_L)\right\| \le \begin{cases} C\left[M^{-2} + N^{-2}(\ln N)^2\right], & \alpha\mu^2 \le \varsigma\varepsilon, \\ C\left[M^{-2} + N^{-2}(\ln N)^3\right], & \alpha\mu^2 \ge \varsigma\varepsilon. \end{cases} \tag{57}$$

The stability of discrete scheme implies

$$\|W_L - w_L\| \le \begin{cases} C\left[M^{-2} + N^{-2}(\ln N)^2\right], & \alpha\mu^2 \le \varsigma\varepsilon, \\ C\left[M^{-2} + N^{-2}(\ln N)^3\right], & \alpha\mu^2 \ge \varsigma\varepsilon. \end{cases} \tag{58}$$

But out of the left boundary layer region, $[\sigma_1, 1-\sigma_2] \cup [1-\sigma_2, 1]$, the absolute error can be calculated using the triangle inequality rule and the bounds of individual components in Lemmas 4 and 13.

$$\begin{aligned} |W_L - w_L| &\le |W_L| + |w_L| \le C\left(N^{-2} + \exp\left(-\frac{\sqrt{\varsigma\alpha}}{\sqrt{\varepsilon}}\,x\right)\right) \le C\left(N^{-2} + \exp\left(-\frac{\sqrt{\varsigma\alpha}}{\sqrt{\varepsilon}}\,\sigma_1\right)\right), \\ |W_L - w_L| &\le C\left(N^{-2} + \exp\left(-\frac{\sqrt{\varsigma\alpha}}{\sqrt{\varepsilon}}\left(\frac{4\sqrt{\varepsilon}}{\sqrt{\varsigma\alpha}}\ln N\right)\right)\right) \le C\left(N^{-2} + N^{-4}\right). \end{aligned} \tag{59}$$

Then, taking the supreme, it implies

$$\|W_L - w_L\| \le CN^{-2}. \tag{60}$$

Equations (58) and (60) give the result. □

Lemma 15. *The right layer component satisfies the following error bound estimate:*

$$\|(W_R - w_R)\| \le \begin{cases} C\left[M^{-2} + N^{-2}(\ln N)^2\right], & \alpha\mu^2 \le \varsigma\varepsilon, \\ C\left[M^{-2} + N^{-2}(\ln N)^2\right], & \alpha\mu^2 \ge \varsigma\varepsilon. \end{cases} \tag{61}$$

Proof. In the right boundary layer region, $[1-\sigma_2, 1]$, if $\alpha\mu^2 \le \varsigma\varepsilon$, then $h_i \le \sqrt{\varepsilon}N^{-1}\ln N$. Otherwise, $h_i \le (1/\mu)N^{-1}\ln N$. The derivative bounds of Lemma 3, singular components bounds of Lemma 4, Lemma 13, and the bound of equation (54) with a similar argument to that of Lemma 14 implies the result. □

Lemma 16. *The regular component satisfies the following error bound estimate:*

$$\|(V - v)\| \le \begin{cases} C\left[M^{-2} + N^{-2}(\ln N)^2\right], & \alpha\mu^2 \le \varsigma\varepsilon, \\ C\left[M^{-2} + N^{-2}(\ln N)^2\right], & \alpha\mu^2 \ge \varsigma\varepsilon. \end{cases} \tag{62}$$

Proof. In the left boundary layer region, $[0, \sigma_1]$, the uniform mesh size, $h_i \le C\sqrt{\varepsilon}N^{-1}\ln N$ if $\alpha\mu^2 \le \varsigma\varepsilon$ or $h_i \le C(\varepsilon/\mu)N^{-1}\ln N$ if $\alpha\mu^2 \ge \varsigma\varepsilon$. Applying the derivative bounds of Lemma 3, the bound of equation (60) becomes

$$\begin{aligned}
\left\|\mathscr{L}_{\varepsilon,\mu}^{M,N}(V-v)\right\| &\le \begin{cases} C\left[M^{-2}+\varepsilon\left(\sqrt{\varepsilon}\,N^{-1}\ln N\right)^2+\mu\left(\sqrt{\varepsilon}\,N^{-1}\ln N\right)^2\right], & \alpha\mu^2 \le \varsigma\varepsilon, \\ C\left[M^{-2}+\varepsilon\left(\dfrac{\varepsilon}{\mu}N^{-1}\ln N\right)^2\left(\varepsilon^2+\mu\varepsilon\right)+\mu\left(\dfrac{\varepsilon}{\mu}N^{-1}\ln N\right)^2(\varepsilon)\right], & \alpha\mu^2 \ge \varsigma\varepsilon, \end{cases} \\
&\le \begin{cases} C\left[M^{-2}+\varepsilon^2N^{-2}(\ln N)^2+\mu\varepsilon N^{-2}(\ln N)^2\right], & \alpha\mu^2 \le \varsigma\varepsilon, \\ C\left[M^{-2}+(\varepsilon+\varepsilon\mu)\dfrac{\varepsilon}{\mu^2}N^{-2}(\ln N)^2+\mu\varepsilon\dfrac{\varepsilon}{\mu^2}N^{-2}(\ln N)^2\right], & \alpha\mu^2 \ge \varsigma\varepsilon, \end{cases} \\
&\le \begin{cases} C\left[M^{-2}+N^{-2}(\ln N)^2\right], & \alpha\mu^2 \le \varsigma\varepsilon, \\ C\left[M^{-2}+N^{-2}(\ln N)^2\right], & \alpha\mu^2 \ge \varsigma\varepsilon. \end{cases}
\end{aligned} \tag{63}$$

Considering the right boundary layer region, $[1-\sigma_2, 1]$, the uniform mesh size, $h_i \le C\sqrt{\varepsilon}N^{-1}\ln N$ if $\alpha\mu^2 \le \varsigma\varepsilon$ or $h_i \le C\mu N^{-1}\ln N$ if $\alpha\mu^2 \ge \varsigma\varepsilon$. We write the bound of equation (60) as

$$\begin{aligned}
\left\|\mathscr{L}_{\varepsilon,\mu}^{M,N}(V-v)\right\| &\le \begin{cases} C\left[M^{-2}+\varepsilon^2N^{-2}(\ln N)^2+\mu\varepsilon N^{-2}(\ln N)^2\right], & \alpha\mu^2 \le \varsigma\varepsilon, \\ C\left[M^{-2}+(\varepsilon+\mu)\mu^2N^{-2}(\ln N)^2+\mu^3N^{-2}(\ln N)^2\right], & \alpha\mu^2 \ge \varsigma\varepsilon, \end{cases} \\
&\le \begin{cases} C\left[M^{-2}+N^{-2}(\ln N)^2\right], & \alpha\mu^2 \le \varsigma\varepsilon, \\ C\left[M^{-2}+N^{-2}(\ln N)^2\right], & \alpha\mu^2 \ge \varsigma\varepsilon. \end{cases}
\end{aligned} \tag{64}$$

The outer boundary layer region, $[\sigma_1, 1-\sigma_2]$ the mesh size, $h_i \le C(2/N^2)$, then

$$\begin{aligned}
\left\|\mathscr{L}_{\varepsilon,\mu}^{M,N}(V-v)\right\| &\le \begin{cases} C\left[M^{-2}+\varepsilon N^{-2}+\mu N^{-2}\right], & \alpha\mu^2 \le \varsigma\varepsilon, \\ C\left[M^{-2}+(\varepsilon+\mu)\mu^2N^{-2}+\varepsilon\mu N^{-2}\right], & \alpha\mu^2 \ge \varsigma\varepsilon, \end{cases} \\
&\le \begin{cases} C\left[M^{-2}+N^{-2}\right], & \alpha\mu^2 \le \varsigma\varepsilon, \\ C\left[M^{-2}+N^{-2}\right], & \alpha\mu^2 \ge \varsigma\varepsilon. \end{cases}
\end{aligned} \tag{65}$$

Combining the three spatial interval cases and applying the maximum principle, we arrive at the required result.

Case II: When $t \in (\tau, T)$

In this case, the approximated values are involved on the right-hand side. Then, the error propagated in these time intervals must be shown, not magnified. We consider the left singular components as

$$\begin{aligned}&\left\|\mathscr{L}_{\varepsilon,\mu}^{M,N}(W_L - w_L) - c_{i,j+1/2}\left((W_L)_{i,j+1-m} - \left(w_L\left(x_i, t_{j+1-m}\right)\right) + (W_L)_{i,j-m} - \left(w_L\left(x_i, t_{j-m}\right)\right)\right)\right\| \\ &\quad \le \left\|\mathscr{L}_{\varepsilon,\mu}^{M,N}(W_L - w_L)\right\| + C\left\|W_L - w_L\right\|.\end{aligned} \tag{66}$$

By Lemma 14,

$$\le \begin{cases} C\left[M^{-2} + N^{-2}(\ln N)^2\right], & \alpha\mu^2 \le \varsigma\varepsilon, \\ C\left[M^{-2} + N^{-2}(\ln N)^3\right], & \alpha\mu^2 \ge \varsigma\varepsilon. \end{cases} \tag{67}$$

Similar arguments can be given for the right layer and outer layer bounds, then Lemma 14 through 16 holds for the whole domain $[0,1] \times [0, T)$. We conclude by the following theorem. □

Theorem 17. *The fitted mesh scheme (38) is $\varepsilon, \mu-$ uniformly convergent under the condition $\alpha\mu^2 \le \varsigma\varepsilon$. The exact solution, u of problem (3) and (4) and approximate solution, U of problem (41) and (42), satisfies the following error estimate.*

$$\|u - U\| \le C\left(N^{-2}(\ln N)^2 + M^{-2}\right). \tag{68}$$

6. Numerical Results and Discussion

Two examples are adopted from [31] for the numerical experiment. Numerical solutions, maximum error estimates, convergence rates, and comparison with prior literature are demonstrated for particular perturbation parameters and mesh grids in graphs and tables.

Example 1

$$-\varepsilon\frac{\partial^2 u}{\partial x^2}(x,t) - \mu(x+1)\frac{\partial u}{\partial x}(x,t) + u(x,t) + \frac{\partial u}{\partial t} = u(x,t-1) - 16x^2(1-x)^2, \quad (x,t) \in (0,1)\times(0,2], \tag{69}$$

subjected to the initial and boundary conditions

$$\begin{cases} u(x,t) = 0, & \forall (x,t) \in (0,1)\times(-1,0], \\ u(0,t) = 0, & \forall t \in (0,2], \\ u(1,t) = 0, & \forall t \in (0,2]. \end{cases} \tag{70}$$

Example 2

$$\begin{aligned}&-\varepsilon\frac{\partial^2 u}{\partial x^2}(x,t) - \mu\left(1 + x(1-x) + t^2\right)\frac{\partial u}{\partial x}(x,t) + (1+5xt)u(x,t) + \frac{\partial u}{\partial t} \\ &\quad = u(x,t-1) - x(1-x)\left(e^t - 1\right), \quad (x,t) \in (0,1)\times(0,2].\end{aligned} \tag{71}$$

subjected to the initial and boundary conditions

$$\begin{cases} u(x,t) = 0, & \forall (x,t) \in (0,1)\times(-1,0], \\ u(0,t) = 0, & \forall t \in (0,2], \\ u(1,t) = 0, & \forall t \in (0,2]. \end{cases} \tag{72}$$

Graphs of numerical solutions applying the developed scheme (41) and (42) for $\varepsilon, \mu = \{10^{-15}, 10^{-20}\}$ are shown in Figures 2 and 3.

The exact solutions of the considered examples are not known. So, the point-wise error estimate and rate of convergence of the proposed scheme are computed using the

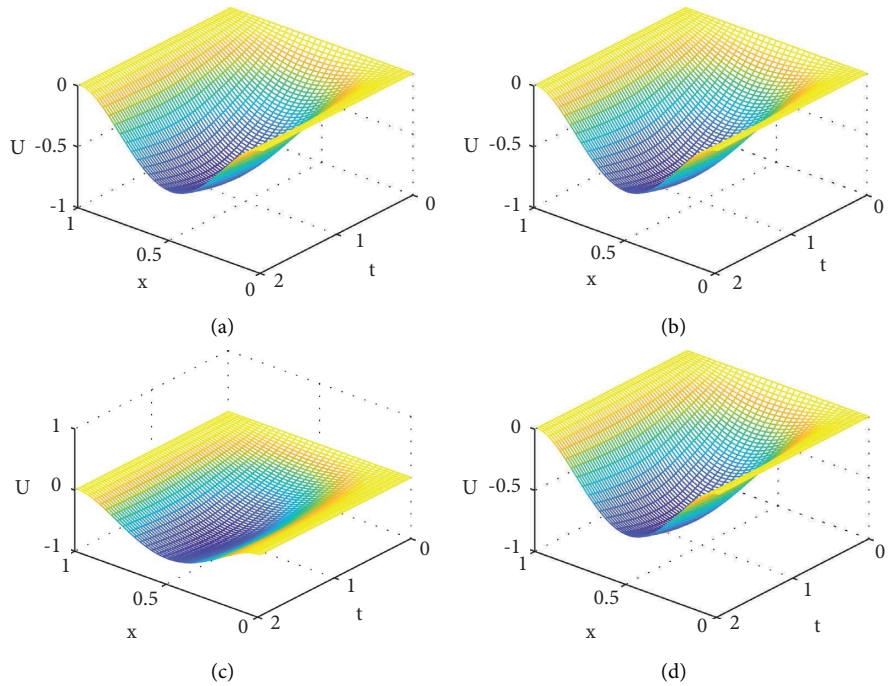

Figure 2: Numerical solutions of Example 1 for some pair of parameters: (a) $[\varepsilon, \mu] = [10^{-15}, 10^{-15}]$, (b) $[\varepsilon, \mu] = [10^{-15}, 10^{-20}]$, (c) $[\varepsilon, \mu] = [10^{-20}, 10^{-15}]$, and (d) $[\varepsilon, \mu] = [10^{-20}, 10^{-20}]$.

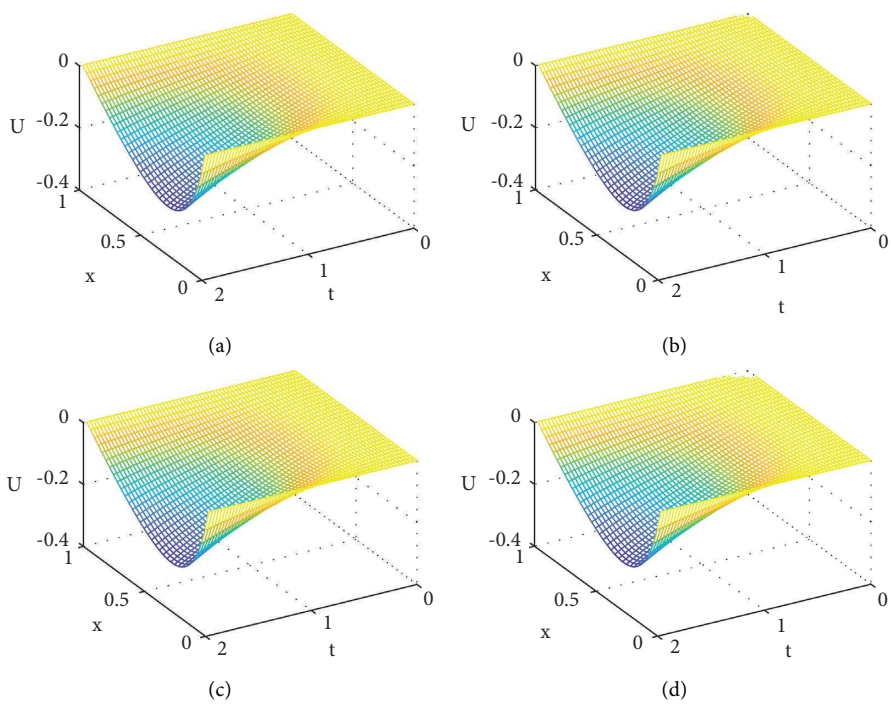

Figure 3: Numerical solutions of Example 2 for some pair of parameters: (a) $[\varepsilon, \mu] = [10^{-15}, 10^{-15}]$, (b) $[\varepsilon, \mu] = [10^{-15}, 10^{-20}]$, (c) $[\varepsilon, \mu] = [10^{-20}, 10^{-15}]$, and (d) $[\varepsilon, \mu] = [10^{-20}, 10^{-20}]$.

Table 1: The error estimate $(E_{\varepsilon,\mu}^{N,M})$ of Example 1, for $\varepsilon = 10^{-20}$.

$\mu\downarrow$	$N = 16$ $M = 16$	32 32	64 64	128 128	256 256	512 512	1024 1024
10^{-13}	$7.7415e-04$	$1.9296e-04$	$4.8221e-05$	$1.2062e-05$	$3.0137e-06$	$1.0266e-06$	$1.1551e-06$
10^{-14}	$7.7415e-04$	$1.9296e-04$	$4.8221e-05$	$1.2062e-05$	$3.0137e-06$	$1.0266e-06$	$1.1551e-06$
10^{-15}	$7.7415e-04$	$1.9296e-04$	$4.8221e-05$	$1.2062e-05$	$3.0135e-06$	$7.5339e-07$	$1.8835e-07$
10^{-16}	$7.7415e-04$	$1.9296e-04$	$4.8221e-05$	$1.2055e-05$	$3.0135e-06$	$7.5339e-07$	$1.8835e-07$
$\vdots$	$\vdots$	$\vdots$	$\vdots$	$\vdots$	$\vdots$	$\vdots$	$\vdots$
10^{-40}	$7.7415e-04$	$1.9296e-04$	$4.8221e-05$	$1.2055e-05$	$3.0135e-06$	$7.5339e-07$	$1.8835e-07$

Table 2: The error estimate $(E_{\varepsilon,\mu}^{N,M})$ of Example 1, for $\mu = 10^{-20}$.

$\varepsilon\downarrow$	$N = 16$ $M = 16$	32 32	64 64	128 128	256 256	512 512	1024 1024
10^{-13}	$7.7415e-04$	$1.9296e-04$	$4.8221e-05$	$1.2062e-05$	$3.0137e-06$	$1.0266e-06$	$1.1551e-06$
10^{-14}	$7.7415e-04$	$1.9296e-04$	$4.8221e-05$	$1.2062e-05$	$3.0137e-06$	$1.0266e-06$	$1.1551e-06$
10^{-15}	$7.7415e-04$	$1.9296e-04$	$4.8221e-05$	$1.2062e-05$	$3.0135e-06$	$7.5339e-07$	$1.8835e-07$
10^{-16}	$7.7415e-04$	$1.9296e-04$	$4.8221e-05$	$1.2055e-05$	$3.0135e-06$	$7.5339e-07$	$1.8835e-07$
$\vdots$	$\vdots$	$\vdots$	$\vdots$	$\vdots$	$\vdots$	$\vdots$	$\vdots$
10^{-40}	$7.7415e-04$	$1.9296e-04$	$4.8221e-05$	$1.2055e-05$	$3.0135e-06$	$7.5339e-07$	$1.8835e-07$

Table 3: The maximum error estimate $(E^{N,M})$ and rate of convergence $(R^{N,M})$ of Example 1, for $10^{-40} \le \varepsilon, \mu \le 10^{-16}$.

	$N = 16$ $M = 16$	32 32	64 64	128 128	256 256	512 512	1024 1024
$E^{N,M}$	$7.7415e-04$	$1.9296e-04$	$4.8221e-05$	$1.2055e-05$	$3.0135e-06$	$7.5339e-07$	$1.8835e-07$
$R^{N,M}$	**2.0043**	**2.0011**	**2.0006**	**2.0001**	**2.0000**	**2.0000**	

Bold values emphasize that it concludes the rate of convergence for any small parameter.

Table 4: The error estimate $(E_{\varepsilon,\mu}^{N,M})$ of Example 2, for $\varepsilon = 10^{-20}$.

$\mu\downarrow$	$N = 16$ $M = 16$	32 32	64 64	128 128	256 256	512 512	1024 1024
10^{-13}	$1.7681e-04$	$4.6676e-05$	$1.2005e-05$	$3.0402e-06$	$7.6487e-07$	$1.9194e-07$	$4.7846e-08$
10^{-14}	$1.7681e-04$	$4.6676e-05$	$1.2005e-05$	$3.0402e-06$	$7.6487e-07$	$1.9194e-07$	$4.7846e-08$
10^{-15}	$1.7681e-04$	$4.6676e-05$	$1.2005e-05$	$3.0402e-06$	$7.6487e-07$	$1.9194e-07$	$4.7846e-08$
10^{-16}	$7.7415e-04$	$1.9296e-04$	$4.8221e-05$	$1.2055e-05$	$3.0135e-06$	$7.5339e-07$	$1.8835e-07$
$\vdots$	$\vdots$	$\vdots$	$\vdots$	$\vdots$	$\vdots$	$\vdots$	$\vdots$
10^{-40}	$1.7681e-04$	$4.6676e-05$	$1.2005e-05$	$3.0402e-06$	$7.6487e-07$	$1.9194e-07$	$4.7846e-08$

Table 5: The error estimate $(E_{\varepsilon,\mu}^{N,M})$ of Example 2, for $\mu = 10^{-20}$.

$\varepsilon\downarrow$	$N = 16$ $M = 16$	32 32	64 64	128 128	256 256	512 512	1024 1024
10^{-13}	$1.7711e-04$	$4.6789e-05$	$1.2204e-05$	$3.2870e-06$	$1.6105e-06$	$1.6182e-06$	$1.6210e-06$
10^{-14}	$1.7711e-04$	$4.6789e-05$	$1.2204e-05$	$3.2870e-06$	$1.6105e-06$	$1.6182e-06$	$1.6210e-06$
10^{-15}	$1.7691e-04$	$4.6712e-05$	$1.2068e-05$	$3.0994e-06$	$8.5175e-07$	$5.1173e-07$	$2.0322e-07$
10^{-16}	$1.7684e-04$	$4.6687e-05$	$1.2025e-05$	$3.0559e-06$	$7.8390e-07$	$2.2347e-07$	$5.8863e-08$
$\vdots$	$\vdots$	$\vdots$	$\vdots$	$\vdots$	$\vdots$	$\vdots$	$\vdots$
10^{-40}	$1.7681e-04$	$4.6676e-05$	$1.2005e-05$	$3.0402e-06$	$7.6487e-07$	$1.9194e-07$	$4.783e-08$

double mesh principle. For each perturbation parameter ε and μ, we set numerical solutions $U_{i.j}$ on a grid mesh $M \times N$ and $\overline{U}_{i,j}$ on a doubled grid mesh $2M \times 2N$. The error estimate of the numerical solution on the discrete parameters N and M, $E_{\varepsilon.\mu}^{N,M}$ is

$$E_{\varepsilon.\mu}^{N,M} = \max_{1\le i\le N 1\le j\le M} \left| U_{i,j} - \overline{U}_{2i-1,2j-1} \right|, \tag{73}$$

and the corresponding rate of convergence, $R_{\varepsilon.\mu}^{M,N}$ is given as

$$R_{\varepsilon.\mu}^{M,N} = \log_2\left(E_{\varepsilon.\mu}^{N,M}\right) - \log_2\left(E_{\varepsilon.\mu}^{2N,2M}\right). \tag{74}$$

Table 6: The maximum error estimate $(E^{N,M})$ and rate of convergence $(R^{N,M})$ of Example 2, for $10^{-40} \le \varepsilon, \mu \le 10^{-16}$.

	$N = 16$	32	64	128	256	512	1024
	$M = 16$	32	64	128	256	512	1024
$E^{N,M}$	$1.7681e-04$	$4.6676e-05$	$1.2005e-05$	$3.0402e-06$	$7.6487e-07$	$1.9194e-07$	$4.783e-08$
$R^{N,M}$	**1.9215**	**1.9591**	**1.9814**	**1.9909**	**1.9946**	**1.9989**	

Bold values emphasize that it concludes the rate of convergence for any small parameter.

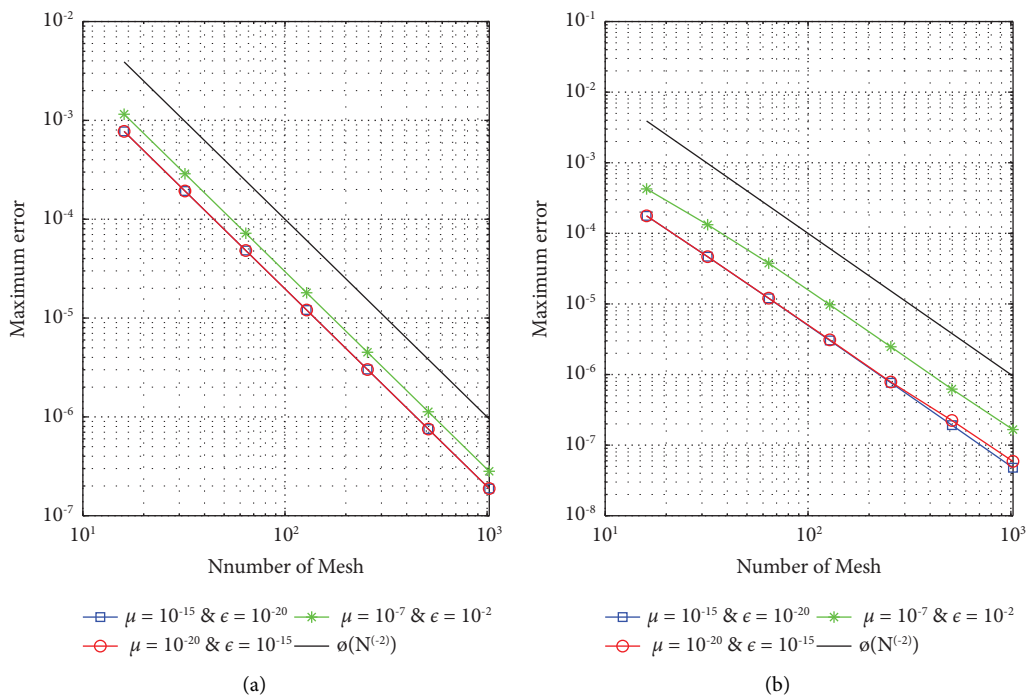

Figure 4: Logarithmic scaled graphs of maximum error versus number of meshes: (a) Example 1 and (b) Example 2.

Table 7: Comparison of the error estimate $(E^{N,M}_{\varepsilon,\mu})$ and rate of convergence $(R^{N,M}_{\varepsilon,\mu})$ of Example 1, for $\varepsilon = 10^{-4}$ and $\mu = 10^{-9}$.

Method	N	32	64	128	256	512
	M	8	16	32	64	128
[32]	$E^{N,M}_{\varepsilon,\mu}$	$4.3817e-02$	$1.670e-02$	$7.4019e-03$	$3.7490e-03$	$1.9008e-03$
	$R^{N,M}_{\varepsilon,\mu}$	1.3875	1.1784	0.9804	0.9798	
[33]	$E^{N,M}_{\varepsilon,\mu}$	$1.4464e-02$	$5{,}6157e-03$	$2.0072e-03$	$6.3177e-04$	$1.8123e-04$
	$R^{N,M}_{\varepsilon,\mu}$	1.3649	1.4843	1.6677	1.8016	
[34], $\theta = 1$	$E^{N,M}_{\varepsilon,\mu}$	$1.9854e-02$	$1.0658e-02$	$5.5313e-03$	$2.8189e-03$	$1.4231e-03$
	$R^{N,M}_{\varepsilon,\mu}$	0.8924	0.9463	0.9725	0.9861	
[34], $\theta = (1/2)$	$E^{N,M}_{\varepsilon,\mu}$	$1.4517e-03$	$3.6060e-04$	$9.0006e-05$	$2.2492e-05$	$5.6226e-06$
	$R^{N,M}_{\varepsilon,\mu}$	2.0092	2.0023	2.0007	2.0001	
The present	$E^{N,M}_{\varepsilon,\mu}$	$3.0452e-02$	$1.9312e-04$	$4.8256e-05$	$1.2064e-05$	$3.0158e-06$
	$R^{N,M}_{\varepsilon,\mu}$	7.3009	2.0007	2.0001	2.0000	

The maximum absolute error, $E^{N,M}$, and the corresponding rate of convergence, $R^{M,N}$, when both ε and μ mutually tend to zero are defined by

$$E^{N,M} = \max_{0<\varepsilon,\mu\ll 1}\left\{E^{N,M}_{\varepsilon,\mu}\right\},$$
$$R^{M,N} = \log_2\left(E^{N,M}\right) - \log_2\left(E^{2N,2M}\right). \tag{75}$$

The error estimate and rate of convergence of numerical solution of the test problems using the given scheme (41), with the considered conditions, fixing one of the perturbation parameters and reducing the other are tabulated in Tables 1 and 2. Table 3 illustrates the maximum error estimate and the corresponding rate of convergence of Example 1. A similar illustration is given through Tables 4–6 for Example 2. The maximum point-wise error decreases uniformly as the number of meshes increase irrespective of perturbation parameters' values with the second order of convergence which is expected from our theoretical result in the previous section. The logarithmic scaled graph in Figure 4 strengthens the predicted convergence rate.

The numerical solution in [34] compared the error and convergence rate of problem 1, when $\varepsilon = 10^{-4}$ and $\mu = 10^{-9}$ for mesh grid $64 \leq N = 4M \leq 512$, with the prior literature results of [32, 33]. We also include our numerical out comes in comparison with these prior results in Table 7.

7. Conclusion

In this study, a numerical method is developed to resolve a one-dimensional parabolic problem with a long time delay and two singularly perturbed parameters. Diffusion and convection terms are multiplied by the perturbation parameters. But we take into account areas where the diffusion term predominates. In the time and spatial dimensions, uniform mesh and piece-wise uniform Shishkin mesh discretization are used, respectively. The Crank–Nicolson method is used to formulate the numerical scheme on two successive time steps, and average central finite differences are used to approximate the spatial derivatives. Under the premise of diffusion-dominant problems ($\alpha\mu^2 \leq \varsigma\varepsilon$), we computationally showed that the approach is uniformly convergent, independent of perturbation parameters. We also validated the numerical solutions of the governing equation by solving two test problems. The maximum point-wise error decreases uniformly independent of perturbation parameters with almost the second order of convergence as the number of meshes doubles, which aligns with the theoretical analysis. The logarithmic scaled graphs in Figure 4 demonstrate the same convergence rate. Although we restrict the method to convective-dominated problems, the formulated scheme is more accurate and efficient compared to numerical methods that exist in prior literature. We focus on diffusion-dominant and one-dimensional problems; one can extend this work to two-dimensional problems and study the other case, conviction-dominant problems.

Data Availability

No data were used to support the findings of this study.

Conflicts of Interest

The authors declare that they have no conflicts of interest.

Acknowledgments

The authors want to thank Arba Minch University for the material and financial support.

References

[1] R. E. O'malley, "Two-parameter singular perturbation problems for second-order equations," *Journal of Mathematics and Mechanics*, vol. 16, pp. 1143–1164, 1967.

[2] M. K. Kadalbajoo and V. Gupta, "Vikas A brief survey on numerical methods for solving singularly perturbed problems," *Applied Mathematics and Computation*, vol. 217, no. 8, pp. 3641–3716, 2010.

[3] X.-W. Gao, Y.-M. Zhu, and T. Pan, "Finite line method for solving high-order partial differential equations in science and engineering," *Partial Differential Equations in Applied Mathematics*, vol. 7, no. 2023, Article ID 100477, 2023.

[4] V. Gupta, M. K. Kadalbajoo, and R. K. Dubey, "A parameter-uniform higher order finite difference scheme for singularly perturbed time-dependent parabolic problem with two small parameters," *International Journal of Computer Mathematics*, vol. 96, no. 3, pp. 474–499, 2019.

[5] M. K. Kadalbajoo and A. S. Yadaw, "Parameter-uniform finite element method for two-parameter singularly perturbed parabolic reaction-diffusion problems," *International Journal of Computational Methods*, vol. 09, no. 04, Article ID 1250047, 2012.

[6] E. O'Riordan, M. Pickett, and G. Shishkin, "Parameter-uniform finite difference schemes for singularly perturbed parabolic diffusion-convection-reaction problems," *Mathematics of Computation*, vol. 75, no. 255, pp. 1135–1155, 2006.

[7] P. Das and V. Mehrmann, "Numerical solution of singularly perturbed convection-diffusion-reaction problems with two small parameters," *BIT Numerical Mathematics*, vol. 56, no. 1, pp. 51–76, 2016.

[8] J. B. Munyakazi, "A robust finite difference method for two-parameter parabolic convection-diffusion problems," *Applied Mathematics and Information Sciences*, vol. 9, p. 2877, 2015.

[9] A. Jha and M. K. Kadalbajoo, "A robust layer adapted difference method for singularly perturbed two-parameter parabolic problems," *International Journal of Computer Mathematics*, vol. 92, no. 6, pp. 1204–1221, 2015.

[10] T. Bullo, G. Duressa, and G. Degla, "Higher order fitted operator finite difference method for two-parameter parabolic convection-diffusion problems," *International Journal of Engineering and Applied Sciences*, vol. 11, no. 4, pp. 455–467, 2019.

[11] A. Das and S. Natesan, "Uniformly convergent hybrid numerical scheme for singularly perturbed delay parabolic convection–diffusion problems on Shishkin mesh," *Applied Mathematics and Computation*, vol. 271, pp. 168–186, 2015.

[12] M. Chandru, T. Prabha, and V. Shanthi, "A parameter robust higher order numerical method for singularly perturbed two parameter problems with non-smooth data," *Journal of Computational and Applied Mathematics*, vol. 309, pp. 11–27, 2017.

[13] T. Prabha, M. Chandru, and V. Shanthi, "Hybrid difference scheme for singularly perturbed reaction-convection-diffusion problem with boundary and interior layers," *Applied Mathematics and Computation*, vol. 314, pp. 237–256, 2017.

[14] T. Prabha, M. Chandru, V. Shanthi, and H. Ramos, "Discrete approximation for a two-parameter singularly perturbed boundary value problem having discontinuity in convection

coefficient and source term," *Journal of Computational and Applied Mathematics*, vol. 359, pp. 102–118, 2019.

[15] M. Chandru, P. Das, and H. Ramos, "Numerical treatment of two-parameter singularly perturbed parabolic convection diffusion problems with non-smooth data," *Mathematical Methods in the Applied Sciences*, vol. 41, no. 14, pp. 5359–5387, 2018.

[16] M. Chandru, T. Prabha, P. Das, and V. Shanthi, "A numerical method for solving boundary and interior layers dominated parabolic problems with discontinuous convection coefficient and source terms," *Differential Equations and Dynamical Systems*, vol. 27, no. 1-3, pp. 91–112, 2019.

[17] M. Kumar, J. Singh, S. Kumar, and A. Aakansha, "A robust numerical method for a coupled system of singularly perturbed parabolic delay problems," *Engineering Computations*, vol. 38, no. 2, pp. 964–988, 2021.

[18] S. Kumar and S. Kumar, "Layer-adapted methods for quasilinear singularly perturbed delay differential problems," *Applied Mathematics and Computation*, vol. 233, pp. 214–221, 2014.

[19] S. Kumar and M. Kumar, "High order parameter-uniform discretization for singularly perturbed parabolic partial differential equations with time delay," *Computers and Mathematics with Applications*, vol. 68, no. 10, pp. 1355–1367, 2014.

[20] A. A. Salama and D. G. Al-Amery, "A higher order uniformly convergent method for singularly perturbed delay parabolic partial differential equations," *International Journal of Computer Mathematics*, vol. 94, no. 12, pp. 2520–2546, 2017.

[21] E. B. M. Bashier and K. C. Patidar, "A second-order fitted operator finite difference method for a singularly perturbed delay parabolic partial differential equation," *Journal of Difference Equations and Applications*, vol. 17, no. 05, pp. 779–794, 2011.

[22] N. A. Mbroh, S. C. Oukouomi Noutchie, and R. Y. M'pika Massoukou, "A robust method of lines solution for singularly perturbed delay parabolic problem," *Alexandria Engineering Journal*, vol. 59, no. 4, pp. 2543–2554, 2020.

[23] M. M. Woldaregay, W. T. Aniley, and G. F. Duressa, "Novel numerical scheme for singularly perturbed time delay convection-diffusion equation," *Advances in Mathematical Physics*, vol. 2021, pp. 1–13, 2021.

[24] V. Gupta, M. Kumar, and S. Kumar, "Higher order numerical approximation for time dependent singularly perturbed differential-difference convection-diffusion equations," *Numerical Methods for Partial Differential Equations*, vol. 34, no. 1, pp. 357–380, 2018.

[25] S. Kumar, S. Kumar, and Sumit, "High-order convergent methods for singularly perturbed quasilinear problems with integral boundary conditions," *Mathematical Methods in the Applied Sciences*, 2014.

[26] M. Kumar and S. Kumar, "High order robust approximations for singularly perturbed semilinear systems," *Applied Mathematical Modelling*, vol. 36, no. 8, pp. 3570–3579, 2012.

[27] S. Kumar, Sumit, and J. Vigo-Aguiar, "A high order convergent numerical method for singularly perturbed time dependent problems using mesh equidistribution," *Mathematics and Computers in Simulation*, vol. 199, pp. 287–306, 2022.

[28] S. Sumit, S. Kumar, and M. Kumar, "Optimal fourth-order parameter-uniform convergence of a non-monotone scheme on equidistributed meshes for singularly perturbed reaction–diffusion problems," *International Journal of Computer Mathematics*, vol. 99, no. 8, pp. 1638–1653, 2022.

[29] A. H. Ejere, G. F. Duressa, M. M. Woldaregay, T. G. Dinka, and T. Gemechu, "A parameter-uniform numerical scheme for solving singularly perturbed parabolic reaction-diffusion problems with delay in the spatial variable," *International Journal of Mathematics and Mathematical Sciences*, vol. 2023, Article ID 7215106, 17 pages, 2023.

[30] A. H. Ejere, G. F. Duressa, M. M. Woldaregay, T. G. Dinka, and T. Gemechu, "A robust numerical scheme for singularly perturbed differential equations with spatio-temporal delays," *Frontiers in Applied Mathematics and Statistics*, vol. 9, Article ID 1125347, 2023.

[31] L. Govindarao, S. R. Sahu, and J. Mohapatra, "Uniformly convergent numerical method for singularly perturbed time delay parabolic problem with two small parameters," *Iranian Journal of Science and Technology Transaction A-Science*, vol. 43, no. 5, pp. 2373–2383, 2019.

[32] S. Kumar, M. Kumar, and Kuldeep, "A robust numerical method for a two-parameter singularly perturbed time delay parabolic problem," *Computational and Applied Mathematics*, vol. 39, pp. 1–25, 2020.

[33] S. Singh, P. Kumari, and D. Kumar, "An effective numerical approach for two parameter time-delayed singularly perturbed problems," *Computational and Applied Mathematics*, vol. 41, no. 8, p. 337, 2022.

[34] M. A. Ayele, A. A. Tiruneh, G. A. Derese, and G. A. Derese, "Fitted cubic spline scheme for two-parameter singularly perturbed time-delay parabolic problems," *Results in Applied Mathematics*, vol. 18, Article ID 100361, 2023.

[35] M. P. Rajan and G. D. Reddy, "A generalized regularization scheme for solving singularly perturbed parabolic PDEs," *Partial Differential Equations in Applied Mathematics*, vol. 5, Article ID 100270, 2022.

[36] J. J. H. Miller, E. O'Riordan, G. I. Shishkin, and L. P. Shishkina, *Fitted Mesh Methods for Problems with Parabolic Boundary Layers*, JSTOR, Ireland, 1998.

[37] S. V. Richard, *Matrix Iterative Analysis*, Springer, Berlin, Germany, 2004.